

See discussions, stats, and author profiles for this publication at: <https://www.researchgate.net/publication/6122554>

# Molecular Dynamic Simulations of Eicosanoic Acid and 18-Methyleicosanoic Acid Langmuir Monolayers

ARTICLE *in* THE JOURNAL OF PHYSICAL CHEMISTRY B · OCTOBER 2007

Impact Factor: 3.3 · DOI: 10.1021/jp073697k · Source: PubMed

---

CITATIONS

12

---

READS

28

## 2 AUTHORS:



[Roger L McMullen](#)

Ashland Specialty Ingredients

26 PUBLICATIONS 162 CITATIONS

SEE PROFILE



[Stephen P Kelty](#)

Seton Hall University

48 PUBLICATIONS 833 CITATIONS

SEE PROFILE

## Molecular Dynamic Simulations of Eicosanoic Acid and 18-Methyleicosanoic Acid Langmuir Monolayers

Roger L. McMullen<sup>†,‡</sup> and Stephen P. Kelty<sup>\*,†</sup>

*Department of Chemistry and Biochemistry, Center for Computational Research, Seton Hall University, South Orange, New Jersey 07079, and International Specialty Products, Wayne, New Jersey 07470*

*Received: May 14, 2007; In Final Form: July 31, 2007*

The conformational and dynamical properties of Langmuir monolayers of 18-methyleicosanoic acid (18-MEA) and the parent material, eicosanoic acid (EA), are compared using molecular dynamics simulations. The effects on various properties, including film thickness, tilt angle, and order parameter, of the methyl group at the 18 position in 18-MEA were investigated as a function of film-packing density. NVT simulations were run as a function of decreasing areal-packing density similar to experimental Langmuir–Blodgett film compressions and expansions. We find that the order parameters and film thickness for 18-MEA monolayers were markedly different from those of EA. The order parameters for methylene groups for both 18-MEA and EA are greater in the middle region of the chain than at the ends in high-density films. This trend becomes reversed in lower density films. Significantly, our simulations show that the order parameters for methylene groups near the CH<sub>3</sub> and carboxyl termini in 18-MEA are comparatively independent of film density in contrast with those of EA. Our findings show that the presence of the methyl group at the 18-position in 18-MEA induces unique intermolecular structural correlations compared to EA.

### Introduction

Recent interest in atomistic simulation of oriented monomolecular thin films at the air–water interface have primarily focused on identifying complex phase behavior and on the conformational ordering of the aliphatic chains as a function of film density and temperature.<sup>1–15</sup> In nearly all systems studied to date, the film materials were either straight chain aliphatic carboxylic acids or lipids. These studies invariably show that the stable equilibrium form of the molecular film exhibits higher order parameters in the middle region of the hydrocarbon tails and comparatively lower order near the ends. Additionally, the tilt angle of the films decreases with increasing film density resulting in an increase in film thickness. The motivation for the present study is to systematically compare the Langmuir film properties of two related molecules to help define the structure–property relationships that exist when the chain undergoes a small structural modification. Molecular dynamic (MD) simulations were undertaken to compare the behavior of eicosanoic acid (EA, HOOC(CH<sub>2</sub>)<sub>18</sub>CH<sub>3</sub>) and 18-methyleicosanoic acid (18-MEA, HOOC(CH<sub>2</sub>)<sub>16</sub>CH(CH<sub>3</sub>)CH<sub>2</sub>CH<sub>3</sub>) monolayers.

The primary distinction between these two molecules is the presence of the methyl group at the 18 position of 18-MEA. Our initial interest in 18-MEA stems from its natural abundance as a covalently bound fatty acid in mammalian hair fibers.<sup>16</sup> It has been well established previously that unsaturation in the hydrocarbon tail affects molecular order, film thickness, and

dynamical properties (e.g., fluidity).<sup>17,18</sup> The presence of side chain constituents has received less attention but is apparently an important factor in 18-MEA's natural selection as a covalently bound monolayer on mammalian hair fiber surfaces. The extent to which the side-chain substituent affects the structural and dynamical properties of the film is likely to depend on the film's molecular density. Consequently, we undertook MD simulation studies in which the density of the film is varied. An MD simulation approach provides a practical and complementary method to investigate the important properties of this important class of material.

In the present study, we conduct NVT simulations for various film-packing densities of EA and 18-MEA, while monitoring key conformational data such as the order parameter, tilt angle, and monolayer thickness. We find that the introduction of a methyl group at the 18-position of a straight chain fatty acid does in fact confer special conformational behavior resulting in increased film thickness and a higher degree of disorder within the chain. However, we also find that the end of the 18-MEA aliphatic chain is less dependent on the packing density than that found for EA. This finding demonstrates very unique behavior of 18-MEA and may provide a possible explanation for its occurrence in nature where it serves as a covalently bound lipid on the surface of mammalian fibers.

### Computational Methods

All MD simulations were performed using GROMACS simulation software<sup>19,20</sup> in conjunction with the GROMOS 96 forcefield,<sup>21</sup> utilizing united-atoms for the methylene and methyl groups. This forcefield has been well validated for phospholipid bilayer systems.<sup>1</sup> NVT simulations (1000 ps) of pre-equilibrated

\* Corresponding author. E-mail: keltyste@shu.edu.

<sup>†</sup> Seton Hall University.

<sup>‡</sup> International Specialty Products.

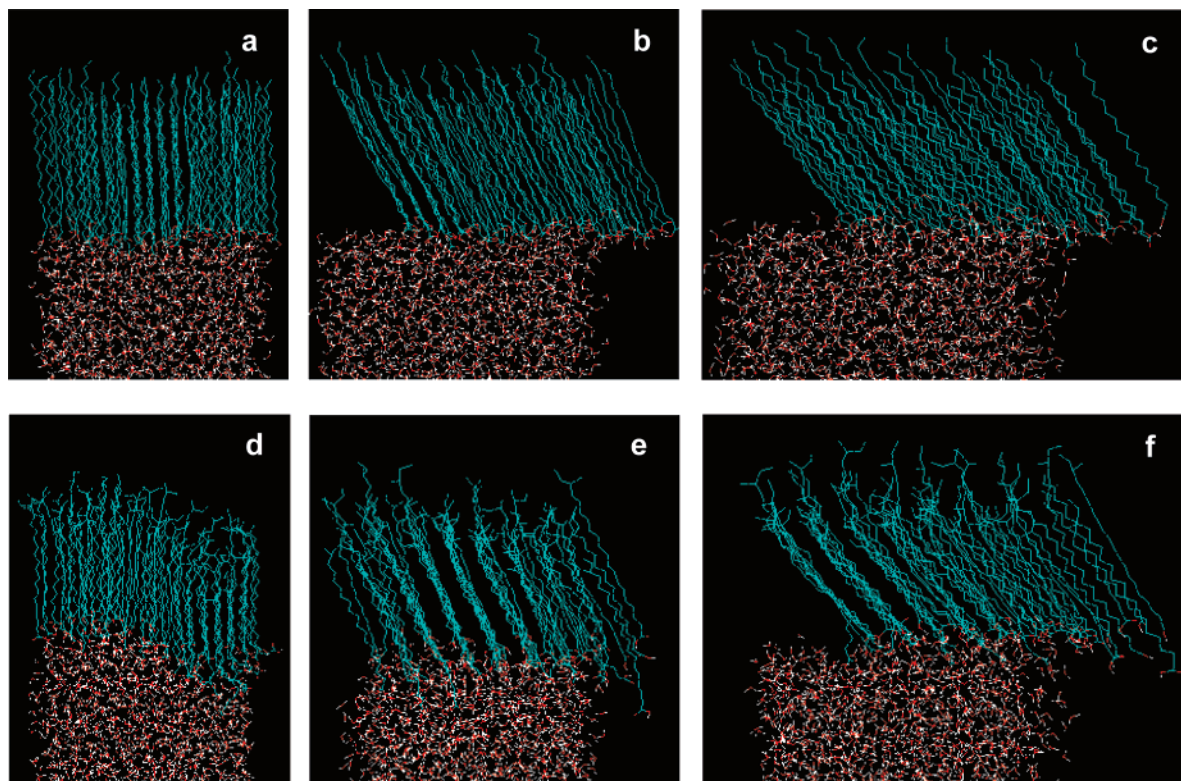


**Figure 1.** MD simulation snapshots for EA (a, b, c) and 18-MEA (d, e, f) at 18.5, 21.5, and 24.5 Å<sup>2</sup>/molecule, respectively.

(400 ps) monolayers were run at each film density starting at 18.5 Å<sup>2</sup>/molecule and incrementing by 0.5 Å<sup>2</sup>/molecule for each successive simulation.<sup>7</sup> The time step in each simulation was 1.0 fs, and the temperature was maintained at 298 K using the Berendsen temperature-coupling method with a time constant of 0.1 ps.<sup>22</sup> Bond lengths were constrained using the SHAKE algorithm<sup>23</sup> for the fatty acids and the SETTLE algorithm<sup>24</sup> for single-point charge (SPC) water. A 0.9 nm cutoff was used for the Lennard-Jones interactions, while long-range electrostatic interactions were treated using the Particle-Mesh Ewald algorithm.<sup>25</sup> All measurements were performed by analysis of the 1000 ps production simulations. To validate the use of 1000 ps simulations for subsequent analysis, we carried out identical simulations for longer time periods up to 5000 ps, and all of the measured parameters remained constant.

Input structure files for MD simulations were based on 64 preoriented monolayer ensembles of either 18-MEA or EA molecules arranged in a hexagonal lattice in an orthorhombic cell. Simulation cells were constructed with a vacuum layer above the aliphatic surface to represent the air–monolayer interface. Below the monolayer was a sufficient number of water molecules (SPC)<sup>26</sup> to achieve a density of 1.0 g/cm<sup>3</sup>. The simulation cells were constructed containing two fatty acid monolayers separated by a 4 nm slab of H<sub>2</sub>O as shown in Figure 1, resulting in a total of 128 fatty acids.<sup>27</sup> This approach prevents water molecules from migrating to any vacuum areas of the simulation box albeit without having to resort to impose position constraints on the solvent mobility although at a slightly higher computational cost. Figure 1a shows a typical cell construction for our input structures.

To probe the structural properties of the materials as a function of film density, successive simulations were run on films in which the initial film density was decreased from 18.5 Å<sup>2</sup>/molecule in 0.5 Å<sup>2</sup>/molecule increments up to 25 Å<sup>2</sup>/molecule. Conformational properties of the monolayer system were analyzed by calculating the deuterium order

parameter, tilt angle, and film thickness as well as other important properties of the system that require monitoring.

## Results and Discussion

The prime motivation of this simulation study was to determine the variations in the structural and dynamical properties of EA and 18-MEA that might lead to the latter material being naturally selected as the uppermost surface in mammalian hair fibers. A major focus of this study is to determine these properties at various film densities because the packing density of 18-MEA on mammalian hair fibers is not well understood at present. Hence, this study is essentially similar to that of expansion of a Langmuir film on an aqueous subphase in which we analyzed the simulation trajectories for monolayer thickness, collective tilt angle, and the deuterium order parameter as a function of packing density in the range 18.5–25 Å<sup>2</sup>/molecule for EA and 18-MEA.

**Monolayer Tilt Angle and Thickness.** It has previously been shown that the tilt angle which Langmuir monolayer chains make with the film normal increases with decreasing packing density.<sup>7,18</sup> Figure 1 shows snapshots from MD simulations of EA and 18-MEA at film densities of 18.5, 21.5, and 24.5 Å<sup>2</sup>/molecule, which demonstrate this effect. Measurements of the tilt angle as a function of film density show that both materials vary smoothly from nearly normal orientation at 18.5 Å<sup>2</sup>/molecule to about 40° from normal at 25 Å<sup>2</sup>/molecule.

The film thickness of EA and 18-MEA as a function of film density is shown in Figure 2. The film thickness was determined from the calculated film density along the *z*-axis of the simulation box. As expected, we observe that the film thickness for each material increases with decreasing tilt angle. It should be noted that at approximately 22 Å<sup>2</sup>/molecule, both systems undergo what appears to be a transition typified by a lower rate of increase. This phenomenon has previously been observed in MD simulations of Langmuir films<sup>7–10</sup> and has been attributed

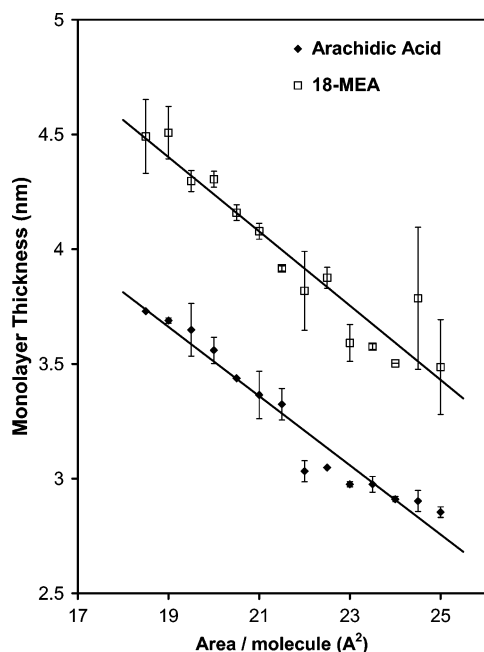


**Figure 2.** Average film thickness for EA (◆) and 18-MEA (□) as a function of film density.

to a phase transition. The factors leading to this phenomenon will be addressed more completely elsewhere. For this study, we note that the plot clearly shows that at each density 18-MEA forms thicker films than EA by about 7–8 Å. In Langmuir films, the film thickness is dependent on the tilt angle and orientational order of the film. Because the tilt angle is essentially the same in each material at a given density, the difference in film thickness for the two materials must be related to the orientational order. This effect is detailed below; however, it can be qualitatively seen from Figure 1 that the 18-MEA film exhibits considerably lower order than EA films. In fact, it appears that some of the 18-MEA molecules have been squeezed out of the monolayer plane, resulting in a greater average film thickness compared to EA. The projecting 18-MEA molecules lead to a broader density profile and correspondingly thicker films presumably due to greater disorder in the film.

**Chain Order.** To monitor the conformation of the fatty acid aliphatic chains, we determined their order relative to an axis normal to the monolayer plane. The orientational order of the chains was determined using a procedure developed by Essex et al., using molecular order tensor parameters for each set of three united atoms:<sup>28</sup>

$$S_{CD} = \frac{2}{3}S_{xx} + \frac{1}{3}S_{yy}$$

where  $S_{xx}$  and  $S_{yy}$  are diagonal elements of the molecular order tensor parameter. Calculated  $S_{CD}$  values can be related to the experimentally determined deuterium order parameter from  $^2\text{H}$  NMR experiments.<sup>29</sup> As with experimentally determined values, greater  $S_{CD}$  values indicate a greater degree of order along the hydrocarbon chain.

In Figure 3,  $S_{CD}$  is plotted as a function of chain position for various packing densities of EA Langmuir films. At higher film densities, we find that  $S_{CD}$  is greater in the middle of the chains and decreases near the headgroup and at the ends of the chains. At lower packing densities, the opposite effect is observed where greater order is found at the end of the chains than in the middle. In the case of 18-MEA, we find a similar pattern (Figure 4); however, this effect is much more pronounced in 18-MEA than

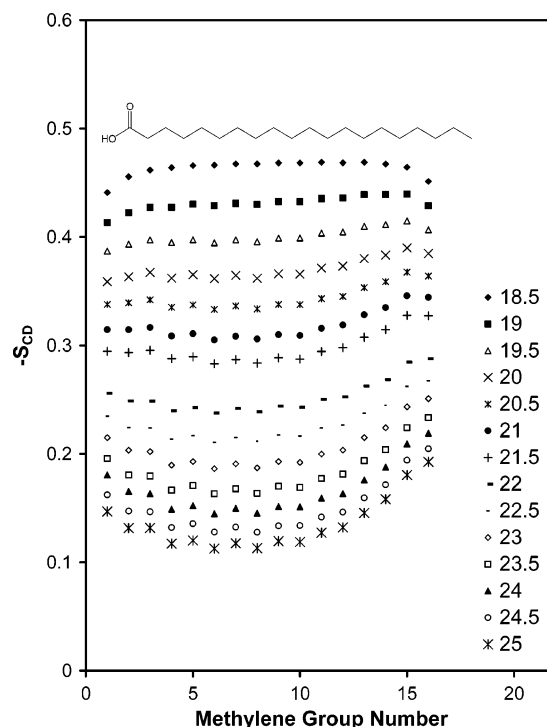


**Figure 3.** Deuterium order parameters  $S_{CD}$  for methylene groups 2 (nearest carboxylate carbon) through 18 for EA for film densities of 18.5–25 Å<sup>2</sup>/molecule as indicated.

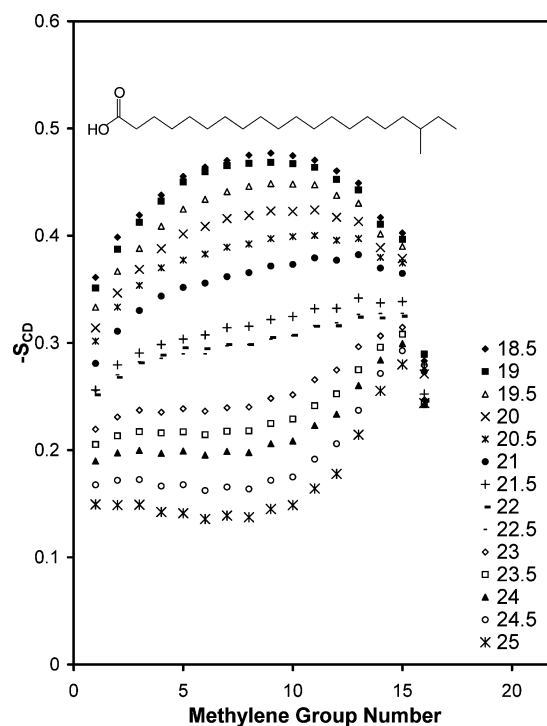


**Figure 4.** Deuterium order parameters  $S_{CD}$  for methylene groups 2 (nearest carboxylate carbon) through 18 for 18-MEA for film densities of 18.5–25 Å<sup>2</sup>/molecule as indicated.

in EA films. In particular, the order parameter for the terminal methyl groups in 18-MEA appear to be considerably less sensitive to film density, adopting approximately the same order parameter of ca. 0.27 ( $\pm 0.02$ ) at all film densities. This result indicates that 18-MEA films appear to adopt an equilibrium structure dominated by the presence of the methyl group at the 18 position. In contrast, terminal methyl  $S_{CD}$  for EA films show a stronger dependence on the film density (0.18–0.45). Signifi-



cantly, there appears to be a single preferred equilibrium structure for 18-MEA that is not observed in other film materials investigated to date.

The average  $S_{CD}$  value for a particular density is indicative of the extent of the molecular tilt angle from normal and of the intramolecular *trans* orientation. Because the tilt angle for 18-MEA and EA is approximately the same for a given film density, the variation in film thickness must have more to do with the intramolecular *trans* orientation than the tilt angle.

The explanation for the unexpected uniformity in order parameter for 18-MEA must be made within the constraints of the interaction forcefield used to produce this result. Our simulations were done using the GROMOS 96 united atom forcefield in which each  $CH_2$  and  $CH_3$  consists of a single, neutral atom type in which the hydrogens are fused to the carbon atoms. Consequently, the observed ordering cannot result from electrostatic or dipole interactions and must result from short range intermolecular van der Waals interactions. Our results indicate that 18-MEA monolayers adopt a unique, ordered minimum energy state in which the bulky 18-methyl groups pack into an orientation that minimizes steric interactions.

In this letter, we report that significant differences arise from the presence of a methyl group at the 18-position of EA in monomolecular thin films. These differences are manifest in the 18-MEA being 0.8 nm thicker at a given density and that this thickness difference is not caused by a simple difference in the film tilt angle, but appears to be reflected in the conformational orientation of the film. The effects that we have observed indicate that the topmost surface of the 18-MEA monolayer, in contrast to EA, appears to adopt a structural motif that is relatively independent of film density. This indicates that 18-MEA films might be capable of exhibiting a chemical or structural resilience to deleterious environmental effects making it more suitable for the exterior surface of mammalian hair fibers which, in turn, could account for its presence in mammalian fibers where the packing density may be highly variable.

**Acknowledgment.** The authors thank Dr. Janusz Jachowicz for useful discussions concerning this work. Support from International Specialty Products, Inc. (R.L.M.) and the New Jersey Commission on Science and Technology (S.P.K.) is acknowledged. This article is dedicated to the memory of the late Roger L. McMullen.

## References and Notes

- (1) Bareman, J. P.; Cardini, G.; Klein, M. L. *Phys. Rev. Lett.* **1988**, *60*, 2152.
- (2) Bareman, J. P.; Cardini, G.; Klein, M. L. *Mater. Res. Soc. Symp. Proc.* **1989**, *141*, 411.
- (3) Bareman, J. P.; Klein, M. L. *J. Phys. Chem.* **1990**, *94*, 5202.
- (4) Cardini, G.; Bareman, J. P.; Klein, M. L. *Chem. Phys. Lett.* **1988**, *145*, 493.
- (5) Duchs, D.; Schmid, F. *J. Phys.: Condens. Matter* **2001**, *13*, 4853.
- (6) Harris, J.; Rice, S. A. *J. Chem. Phys.* **1988**, *89*, 5898.
- (7) Karaborni, S. *Langmuir* **1993**, *9*, 1334.
- (8) Karaborni, S.; Toxvaerd, S. *J. Chem. Phys.* **1992**, *96*, 5505.
- (9) Karaborni, S.; Toxvaerd, S. *J. Chem. Phys.* **1992**, *97*, 5876.
- (10) Karaborni, S.; Toxvaerd, S.; Olsen, O. H. *J. Phys. Chem.* **1992**, *96*, 4965.
- (11) Kim, K. S.; Moller, M. A.; Tildesley, D. J.; Quirke, N. *Mol. Simul.* **1994**, *13*, 77.
- (12) Opps, S. B.; Yang, B.; Gray, C. G.; Sullivan, D. E. *Phys. Rev. E* **2001**, *63*, 41602.
- (13) Pal, B.; Modak, S.; Datta, A. *Surf. Sci.* **1994**, *310*, 407.
- (14) Polimeno, A.; Marijin Ros, J.; Levine, Y. K. *J. Chem. Phys.* **2001**, *115*, 6185.
- (15) Schmid, F.; Stadler, C.; Lange, H. *Colloids Surf., A* **1999**, *149*, 301.
- (16) Jones, L. N.; Rivett, D. E. *Micron* **1997**, *28*, 469.
- (17) Gaines, G. L. *Insoluble Monolayers at Liquid-Gas Interfaces*; Interscience Publishers: New York, 1966.
- (18) Ulman, A. *An Introduction to Ultrathin Organic Films*; Academic Press: London, 1991.
- (19) Berendsen, H. J. C.; van der Spoel, D.; van Drunen, R. *Comput. Phys. Commun.* **1995**, *91*, 43.
- (20) Lindahl, E.; Hess, B.; van der Spoel, D. *J. Mol. Mod.* **2001**, *7*, 306.
- (21) van Gunsteren, W. F.; Billeter, S. R.; Eising, A. A.; Hünenberger, P. H.; Krüger, P.; Mark, A. E.; Scott, W. R. P.; Tironi, I. G. *Biomolecular Simulation: The GROMOS96 manual and user guide*; Hochschulverlag AG an der ETH Zürich: Zürich, Switzerland, 1996.
- (22) Berendsen, H. J. C.; Postma, J. P. M.; DiNola, A.; Haak, J. R. *J. Chem. Phys.* **1984**, *81*, 3684.
- (23) Ryckaert, J. P.; Ciccotti, G.; Berendsen, H. J. C. *J. Comp. Phys.* **1977**, *23*, 327.
- (24) Miyamoto, S.; Kollman, P. A. *J. Comput. Chem.* **1992**, *13*, 952.
- (25) Darden, T.; York, D.; Pedersen, L. *J. Chem. Phys.* **1993**, *98*, 10089.
- (26) Berendsen, H. J. C.; Postma, J. P. M.; van Gunsteren, W. F.; Hermans, J. Interaction models for water in relation to protein hydration. In *Intermolecular Forces*; Pullman, B., Ed.; D. Reidel Publishing Company: Dordrecht, The Netherlands, 1981; pp 331.
- (27) Ahlstrom, P.; Berendsen, H. J. C. *J. Phys. Chem.* **1993**, *97*, 13691.
- (28) Essex, J. W.; Hann, M. M.; Richards, W. G. *Phil. Trans. Roy. Soc. London, Ser. B* **1994**, *344*, 239.
- (29) Seelig, A.; Seelig, J. *Biochemistry* **1974**, *13*, 4839.